COMPARISON OF THE TEMPERATURE COEFFICIENTS OF THE BASIC
I-V PARAMETERS FOR VARIOUS TYPES OF SOLAR CELLS

C. R. Osterwald
Solar Energy Research Institute
Golden, Colorado 80401

T. Glatfelter and J. Burdick
Energy Conversion Devices, Inc.
Troy, Michigan 48084

ABSTRACT

It is well-known that the maximum power output of photovoltaic devices changes with temperature. Therefore, the temperature coefficients of the basic device performance parameters (open-circuit voltage, short-circuit current, fill factor, and efficiency) are important factors which must be taken into account in the design of a photovoltaic power system, where temperature changes occur throughout the day and year. This paper reports results of experimental temperature coefficient measurements obtained on a wide variety of different photovoltaic devices, many of which have not had temperature coefficient data published previously.

INTRODUCTION

It is well-known that photovoltaic device performance, and therefore solar cell maximum power output, changes with temperature. Hence, it is important to take into account the temperature coefficients of the basic device I-V parameters (open-circuit voltage, short-circuit current, fill factor, and efficiency or maximum power point) when designing photovoltaic power systems for actual outdoor applications, where temperature changes occur throughout the day and year. In the past, however, very little temperature coefficient data for devices other than crystalline silicon or GaAs has been published. The objective of this work is to present a comparison of temperature coefficient data for a variety of different solar cell types, several of which have not been previously published. The data is experimentally obtained and is tabulated in both actual parameter units (mV, mA, mW) per degree Celcius, as well as parts-per-million per degree Celcius to enable comparison of the different photovoltaic devices.

MEASUREMENT METHOD

The temperature coefficients for each device were determined from the slope of each I-V parameter versus temperature. All temperature coefficient data measured in this work was obtained using a high-resolution I-V measurement system which has been described elsewhere [1]. The illuminated I-V measurements were performed under a calibrated Spectrolab X-25 solar simulator, and the temperature of the devices was fixed to within +0.1°C with a feedback-controlled thermoelectric plate. The plate temperature was set using a platinum-RTD surface temperature probe which had a resolution of 0.1°C. Since most of the devices did not have bonded contacts, four-terminal Kelvin probe connections were made to each device. The I-V curve was then measured at 5°C (+0.2°C) intervals over a temperature range from 15°C to 60°C without disturbing the contacts (the probe connections). This procedure ensured that any changes in the cell I-V parameters (especially the fill factor) were due solely to the temperature change. For each temperature scan a linear least-squares fit of the Jsc, Voc, FF, and Pmax data was then performed to obtain the slope and correlation coefficient. Typically, the correlation coefficients were within 0.005 of unity; for example, the correlation coefficients of the linear fits for the Voc and Isc measurements were generally within +.003 of unity, while the fill factor correlation coefficients were in the range of 0.994 to 0.996. For comparison purposes, the data and the slopes were then normalized to the 25°C value of the linear fit.

DISCUSSION AND RESULTS

Tables 1 and 2 show a summary of the results for the various photovoltaic devices measured and they include measurements reported in references 2 and 3. In Table 1 the temperature coefficient of each measurement is listed without normalization, and in Table 2 the normalized temperature coefficients are compared, along with previously published data. Figures 1-8 show the results of the device I-V parameters versus temperature (normalized to the linear fit at 25°C) for, respectively: crystalline Si (Fig. 1), ITO/InP (Fig. 2), CuInSe$_2$/Cd(Zn)S (Fig. 3), GaAs double heterostructure (Fig. 4), a-Si alloy single-cell (Fig. 5), a-Si:Ge alloy single-cell (Fig. 6), a-Si alloy same-gap two-cell tandem (Fig. 7), and a-Si:Ge alloy dual-gap two-cell tandem (Fig. 8).

All of the different devices show a decrease in Voc, and an increase in Jsc, with increasing temperature, as expected. However, the most notable feature of these measurements is the results for the amorphous silicon (a-Si) alloy solar cells. All of these devices exhibit a non-linear behavior of the FF and Pmax versus temperature. In addition, the results show the

fill factor with a non-linear positive temperature coefficient (FF increasing with temperature over the range 15°C to 60°C) for the a-Si alloy solar cells, in contrast with a negative FF temperature coefficient for all of the crystalline devices. This positive FF temperature coefficient, in turn, results in very low (least negative) Pmax temperature coefficients of -1000 to -2000 ppm/°C for the a-Si alloy devices, compared to the larger (more negative) Pmax temperature coefficients for the other types of solar cells, most of which range from -2000 to -6000 ppm/°C. These trends, as well as the non-linear FF and Pmax temperature coefficients of the a-Si alloy devices, can be observed from the tables and figures.

In terms of actual outdoor applications, therefore, these I-V versus temperature results mean that the a-Si alloy solar cells will show less decrease in Pmax with increasing temperature than will the other types of (crystalline) photovoltaic devices tested. Finally, from the behavior exhibited by the various types of solar cells that were measured in this study, note that the devices with larger band gaps generally have lower Pmax temperature coefficients than do the narrow band gap solar cells.

Table 1. Temperature coefficient measurement results of the I-V parameters Voc, Jsc, FF, and Pmax, for various types of photovoltaic devices.

Device	$\dfrac{dVoc}{dT}$ (mV/°C)	$\dfrac{dJsc}{dT}$ (mA/cm^2 °C) ($\times 10^{-3}$)	$\dfrac{dFF}{dT}$ (1/°C) ($\times 10^{-4}$)	$\dfrac{dPmax}{dT}$ (mW/cm^2 °C) ($\times 10^{-2}$)
RF Sputtered ITO/InP	-2.39	+10.14	-12.98	-6.79
DC Sputtered ITO/InP	-2.51	+17.98	- 5.97	-5.16
Si MINP [2]	-1.98	+17.1	- 8.57	-5.36
Si passivated emitter [3]	-1.933	+23.4	- 7.55	-6.04
CuInSe$_2$/Cd(Zn)S	-2.01	+ 8.11	-11.66	-5.68
GaAs double heterostructure	-2.42	+ 7.10	- 5.58	-5.63
1.7eV AlGaAs	-2.20	+14.82	- 5.42	-2.44
a-Si:H:F alloy ITO/pin/SS	-2.86	+14.39	+ 8.35 (*)	-0.875 (*)
a-Si:Ge:H:F alloy ITO/pin/SS	-2.84	+25.0	+ 9.82 (*)	-0.766 (*)
a-Si/a-Si alloy ITO/pin/pin/SS	-5.80	+ 7.07	+ 5.98 (*)	-1.395 (*)
a-Si/a-Si:Ge alloy ITO/pin/pin/SS	-5.57	+ 7.88	+ 6.27 (*)	-1.748 (*)

(*) non-linear

Table 2. Normalized temperature coefficients (ppm/^{o}C) of the I-V parameters Voc, Jsc, FF, and Pmax, for various types of photovoltaic devices.

| Device	$\dfrac{1}{Voc}\dfrac{dVoc}{dT}$	$\dfrac{1}{Jsc}\dfrac{dJsc}{dT}$	$\dfrac{1}{FF}\dfrac{dFF}{dT}$	$\dfrac{1}{Pmax}\dfrac{dPmax}{dT}$
Si space cells [2]	-4510 to -3490	380 to 710	-1600 to -1000	-5350 to -4070
GaAs space cells [2]	-2160 to -2040	520 to 710	-1000 to - 610	-2650 to -1950
Si MINP [2]	-3010	580	-1090	-3510
Si passivated emitter [3]	-2960	650	- 940	-3200
RF Sputtered ITO/InP	-3000	370	-1790	-4330
DC Sputtered ITO/InP	-3630	660	- 840	-3820
CuInSe$_2$/Cd(Zn)S	-4580	260	-1720	-5870
GaAs double heterostructure	-2400	300	- 660	-2740
1.7eV AlGaAs	-1810	950	- 650	-1550
a-Si:H:F alloy ITO/pin/SS	-3100 to -3040	830 to 950	320 to 1310 (*)	-1970 to - 980 (*)
a-Si:Ge:H:F alloy ITO/pin/SS	-3890 to -3810	1010 to 1350	990 to 1760 (*)	-1970 to -1020 (*)
a-Si/a-Si alloy ITO/pin/pin/SS	-3270 to -3110	620 to 960	840 to 1580 (*)	-1430 to -1220 (*)
a-Si/a-Si:Ge alloy ITO/pin/pin/SS	-3680 to -3320	720 to 850	930 to 1180 (*)	-1940 to -1660 (*)

(*) non-linear
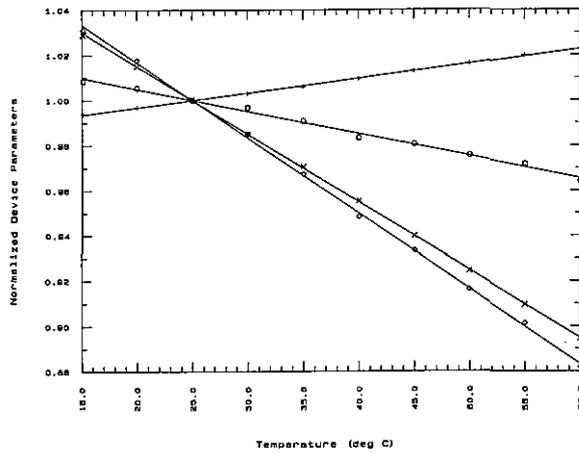
Figure 1. Normalized Voc (X), Jsc (+), FF (0), and Pmax (◇) vs temperature for a high efficiency crystalline silicon photovoltaic device.
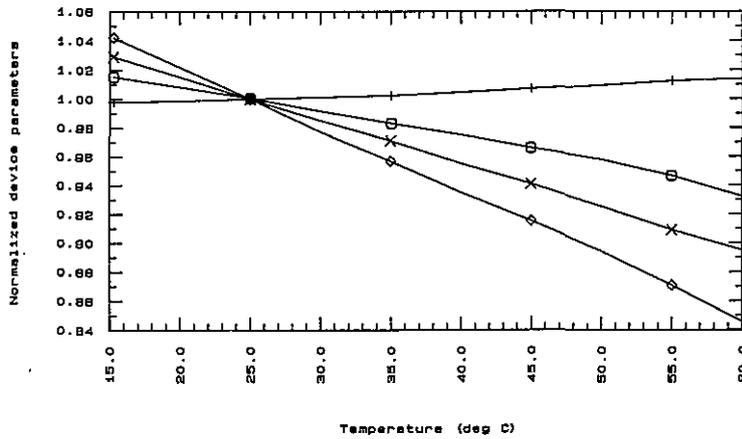

Figure 2. Normalized Voc (X), Jsc (+), FF (0), and Pmax (◇) vs temperature for an ITO/InP photovoltaic device.
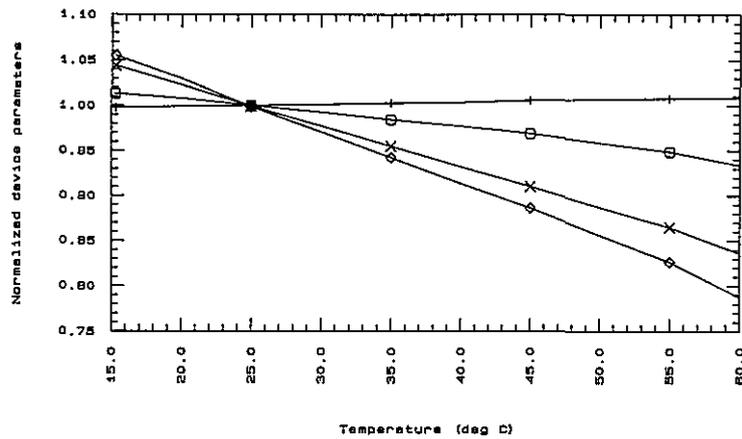

Figure 3. Normalized Voc (X), Jsc (+), FF (0), and Pmax (◇) vs temperature for a CuInSe$_2$/Cd(Zn)S photovoltaic device.
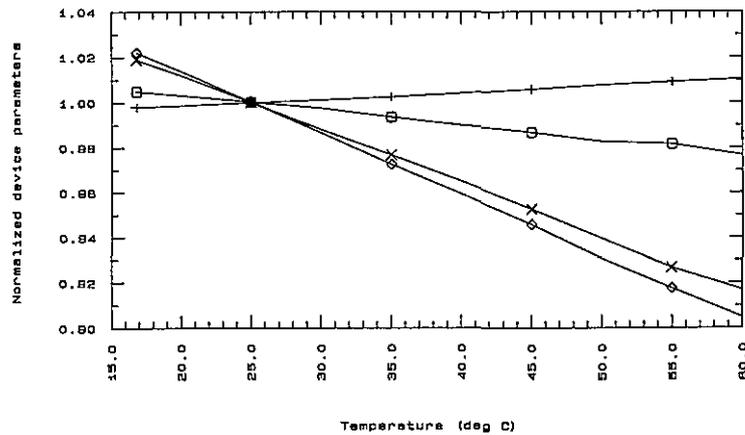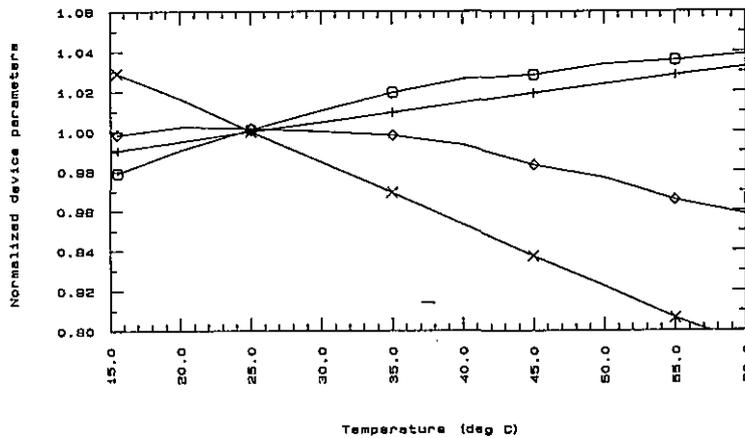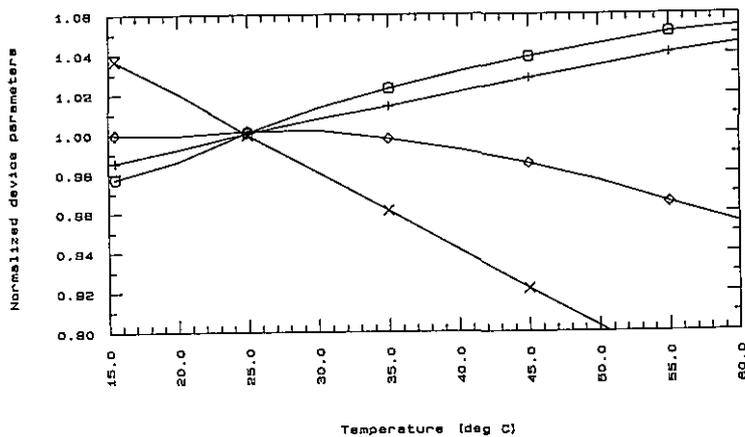
Figure 4. Normalized Voc (X), Jsc (+), FF (0), and Pmax (◇) vs temperature for a GaAs double heterostructure photovoltaic device.

Figure 5. Normalized Voc (X), Jsc (+), FF (0), and Pmax (◇) vs temperature for an a-Si:H:F alloy ITO/pin/SS photovoltaic device.

Figure 6. Normalized Voc (X), Jsc (+), FF (0), and Pmax (◇) vs temperature for an a-Si:Ge:H:F alloy ITO/pin/SS photovoltaic device.
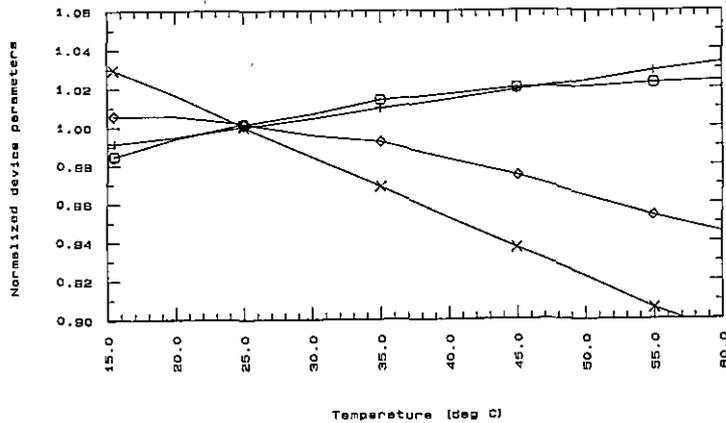
192

Figure 7. Normalized Voc (X), Jsc (+), FF (O), and Pmax (◇) vs temperature for an a-Si/a-Si alloy ITO/pin/pin/SS photovoltaic device.
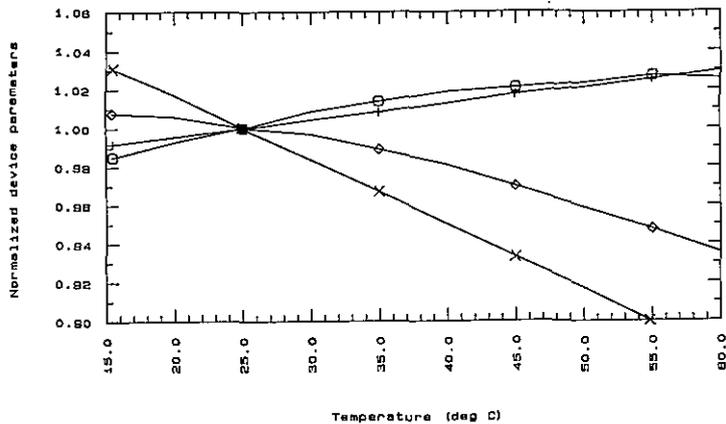

Figure 8. Normalized Voc (X), Isc (+), FF (O), and Pmax (◇) vs temperature for an a-Si/a-Si:Ge alloy ITO/pin/pin/SS photovoltaic device.

ACKNOWLEDGEMENTS

REFERENCES

1. K. A. Emery and C. R. Osterwald, "Solar Cell Efficiency Measurements," Solar Cells, Vol. 17 (1986) p. 253.

2. M. A. Green, K. A. Emery, and A. W. Blakers, "Silicon Solar Cells with Reduced Temperature Sensitivity," Electronics Letters, Vol. 18 (1982) p. 97.

3. M. A. Green, A. W. Blakers, C. R. Osterwald, "Characterization of High-efficiency Silicon Solar Cells," Journal of Applied Physics, Vol. 58 (1985) p.4402.